

Symmetric Cell with LiMn₂₀4 for Aqueous Lithium-ion Battery

Park, Sun-Il
Interdisciplinary Graduate School of Engineering Science, Kyushu University

Okada, Shigeto
Institute for Materials Chemistry and Engineering, Kyushu University

Yamaki, Jun-ichi
Institute for Materials Chemistry and Engineering, Kyushu University

<https://hdl.handle.net/2324/19003>

出版情報 : Journal of Novel Carbon Resource Sciences. 3, pp.27-31, 2011-02. Kyushu University G-COE program "Novel Carbon Resource Sciences" secretariat

バージョン :

権利関係 :

Symmetric Cell with LiMn_2O_4 for Aqueous Lithium-ion Battery

Sun-Il Park^{*1}, Shigeto Okada^{*2}, Jun-ichi Yamaki^{*2}

^{*1}Interdisciplinary Graduate School of Engineering Science, Kyushu University

^{*2}Institute for Materials Chemistry and Engineering, Kyushu University

(Received December 20, 2010; accepted January 31, 2011)

The electrochemical characteristics of LiMn_2O_4 in aqueous electrolyte solutions have been investigated with respect to its use as both the cathode and anode active materials in a new type rechargeable battery system. The results of cyclic voltammetry show that LiMn_2O_4 reversibly intercalated/deintercalated Li^+ ions at potentials below the potentials of hydrogen and oxygen evolution in a neutral aqueous solution. Thus, it could be used as both the cathode and anode in an aqueous battery system without causing the electrolysis of water. The capacity obtained by this cell system is about 110 mAh/g, based on the mass of the cathode, and the rate capability in the aqueous electrolyte was superior to that in organic electrolyte. This new technology solves some major problems of safety, cost and conductivity connected with organic electrolyte and will provide a new strategy to explore advanced energy storage and conversion systems.

1. Introduction

The exhaustion of fossil fuel and the actualizing global warming have strongly encouraged us to search for energy alternatives. A Hybrid Electric Vehicle (HEV) and Electric Vehicle (EV) are significant topics addressing the above problems, and much effort has been devoted to research on advanced batteries for HEV/EVs¹⁻⁹. A lithium ion battery (LIB) with the highest energy density is one of the strongest battery candidates for HEV/EVs on the secondary battery market. However, a total replacement of ignition engines with secondary LIB in the automotive industry is hampered by severe problems such as safety, cost performance and rate capability. LIB contains flammable organic electrolytes, which might cause the production of intense smoke or even fire in the case of improper use such as overcharging or short-circuiting. In addition, the use of costly organic electrolytes and strict humidity control of the assembling environment makes LIB comparatively expensive, and the ion conductivity of the organic electrolytes is generally much lower than that of aqueous electrolytes. There is a clear need

for less expensive and environmentally benign energy storage materials and devices, such as a rechargeable lithium ion battery capable of operating with an aqueous electrolyte¹⁰⁻¹⁷.

The most important item to consider in the development is the proper selection of cathode and anode active materials, due to the decomposition of water. An aqueous LIB has been utilized with LiMn_2O_4 and VO_2 as electrode materials and 5 mol/dm³ LiNO_3 in water as the electrolyte^{14,15}. Since this first report, about 15 papers dedicated to the aqueous LIB have been published. Four -volt class cathodes such as LiMn_2O_4 were used in most of these batteries. As candidates for the electrode material, the LiMn_2O_4 is attractive for many reasons, including its rare-metal-free composition, low cost and abundance as a resource as well as the fact that it causes no environmental pollution. In this study, we report on the performance of an aqueous rechargeable lithium-ion cell with LiMn_2O_4 . Fig. 1 shows the relationship between the potential of several common Li intercalation compounds and the stability limits versus pH for water. The potentials are compared to both Ag/

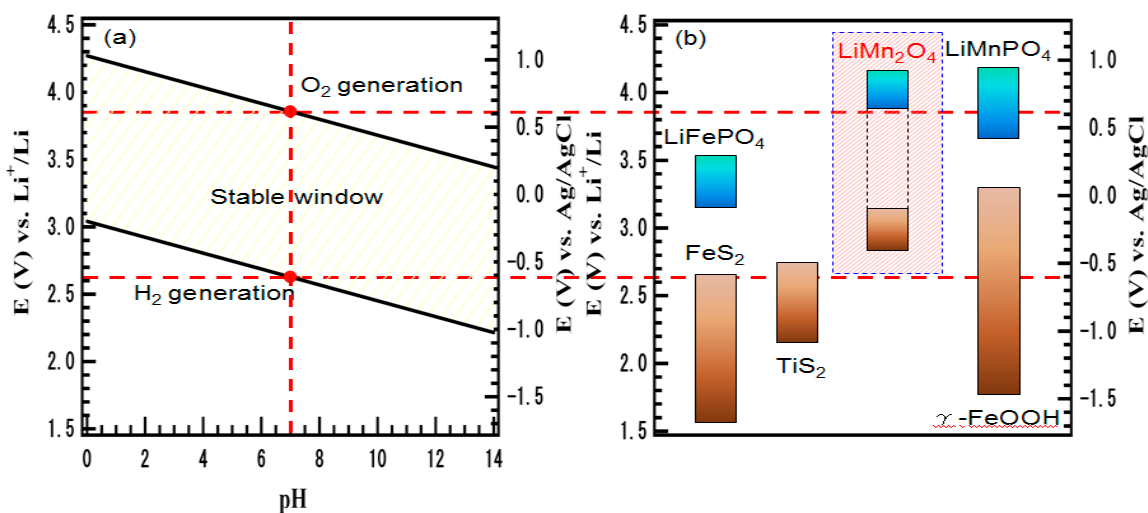


Fig. 1 Electrochemical stability window for water and lithium reaction potential for several materials in a lithium-ion battery.

AgCl potential and Li/Li⁺ potential. At potentials above the stability window of water, oxygen can be generated, whereas at potentials below the stability window, hydrogen evolution can occur (due to an overpotential at the electrodes, the actual evolution potentials of H₂ and O₂ can be shifted to lower and higher values, respectively, and the cell can be operated at a higher voltage). It is obvious that LiMn₂O₄ is a suitable candidate for the cathode and anode material in the aqueous cell.

The aqueous lithium ion cell with LiMn₂O₄ as both the cathode and anode was first considered by Li *et al.*¹⁵. The benefit of the spinel LiMn₂O₄ comes from the two voltage plateaus at 3 and 4 V vs. Li that the material possesses, both of them located in the electrochemical window of aqueous electrolyte. Therefore, LiMn₂O₄ could be utilized as both the cathode and anode in such an aqueous cell. However, to the best of our knowledge, there are no detailed experimental results published in scientific literature concerning the charge/discharge profile and the cell performances of a Li_{1-x}Mn₂O₄//Li_{1+x}Mn₂O₄ aqueous symmetric cell. We focused on the performance of the aqueous rechargeable lithium-ion cell with LiMn₂O₄.

2. Experimental

The sol-gel process was adopted for the synthesis of LiMn₂O₄¹⁸. Stoichiometric amounts of CH₃COOLi·2H₂O (Wako Pure Chemical Industries, Ltd., Japan) and (CH₃COO)₂Mn·4H₂O (Nacalai Tesque, Inc., Japan) with the cationic ratio of Li:Mn = 1:2 were dissolved in distilled water and mixed well with an aqueous solution of adipic acid (Kanto chemical Co. Inc., Japan). Adipic acid was used as a chelating agent to produce a gel in the molar ratio of adipic acid to total metal ions of 1:1. The solution was evaporated at 90 °C, and after 12 h a transparent sol was obtained. The resultant sol was additionally dried at 90-100 °C for 24 h in a vacuum dryer to yield gel precursors. These gel precursors were consequently decomposed at 300 °C for 10 h in air to eliminate organic contents. The decomposed powders were ground and calcined at 800 °C for 10 h in air to obtain highly crystalline LiMn₂O₄ powders. Powder X-ray diffraction (XRD, Rigaku, RINT 2100HLR/PC) with CuKα radiation was used to examine the crystalline phase of the prepared material from 2θ = 10°-80° at a 2.0 °/s scan rate. Electrodes for the electrochemical studies were fabricated with active material, acetylene black (Denki Kagaku Co.) as the conducting additive and polytetrafluoroethylene (PTFE-Daikin Industries, Ltd.) as the binder at a weight ratio of 70:25:5 for the cathode and anode, respectively.

Cyclic voltammetry (CV) was accomplished using a three-electrode cell in a 2 mol/dm³ Li₂SO₄ solution, with platinum and a silver-silver chloride electrode (Ag/AgCl, E = 0.222 V vs. standard hydrogen electrode, NHE) as the counter and reference electrodes, respectively. CV was performed using a Voltalab potentiostat Model PGZ 402 electrochemical interface, controlled by a computer. Galvanostatic discharge and charge tests were carried out with a cycler (NAGANO BTS-2004W) at a constant current density. The cathode (about 30 mg) and anode electrode disks were punched into Ni mesh and immersed

in 2 mol/dm³ Li₂SO₄ solution; the distance between the electrodes was kept at about 1 cm. The electrochemical properties of Li_{1-x}Mn₂O₄//Li_{1+x}Mn₂O₄ were also tested in an organic electrolyte cell by using a 1 mol/dm³ LiPF₆/EC:DMC (1:1 vol%) electrolyte. All electrical measurements were performed at ambient temperature.

3. Results and discussion

The X-ray diffraction (XRD) pattern of as-synthesized crystalline LiMn₂O₄ is shown in Fig. 2. The synthesized LiMn₂O₄ powder was indexed as the spinel phase belonging to the Fd3m space group, where Li atoms occupy tetragonal 8a sites, Mn atoms occupy octahedral 16d sites and O atoms occupy 32e sites, respectively. The crystal lattice parameter (a = 8.239 Å) was close to that of stoichiometric LiMn₂O₄ spinel (8.245 Å)¹⁹, and the XRD pattern was consistent with ICDD-35-0782. The cyclic voltammogram of the current collector, a Ni mesh electrode, was measured in 2 mol/dm³ Li₂SO₄ solution and is shown in Fig. 3. The potential window of water was determined based on the electrolysis potential, which means the H₂ and O₂ evolution at the negative and positive potentials, respectively. In an aqueous system, the H₂ and O₂ gas evolution occur according to the following equations²⁰.

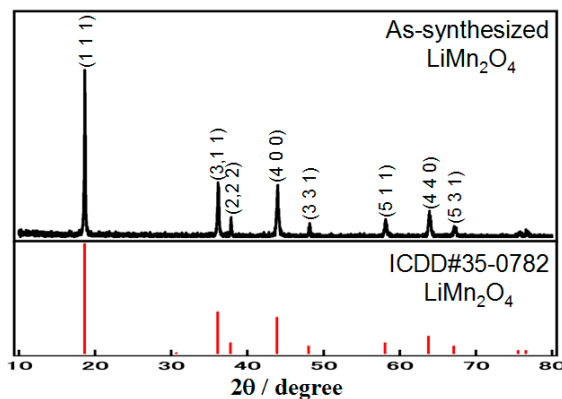
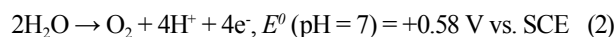
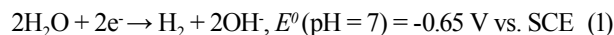


Fig. 2 XRD pattern of LiMn₂O₄.

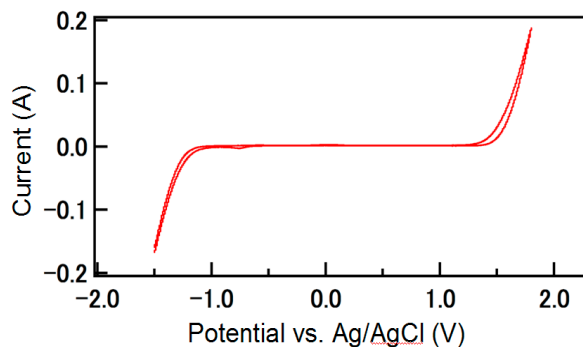
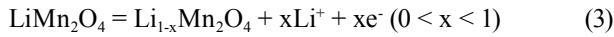
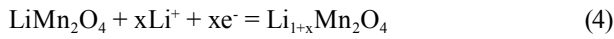


Fig. 3 Cyclic voltammogram for Ni electrode in 2 mol/dm³ Li₂SO₄ aqueous solution (scan rate 10 mV/s).

The theoretically stable voltage limit is 1.23 V. In the case of $2 \text{ mol/dm}^3 \text{ Li}_2\text{SO}_4$ solution, two peaks should be observed, the positive-going peak at about 1.5 V (versus Ag/AgCl) and the negative-going one at about -1.0 V corresponding to O_2 and H_2 generation, respectively. Therefore, the stable electrochemical window of the solution is about 2.5 V, which is much larger than that of pure water (1.23 V), due to large overpotentials. Therefore, the materials used as electrodes in aqueous electrolytes must maintain excellent stability during the electrochemical process in a water-based lithium salt solution. The cyclic voltammograms of the prepared LiMn_2O_4 electrode in $2 \text{ mol/dm}^3 \text{ Li}_2\text{SO}_4$ aqueous electrolyte at a scan rate of 0.5 mV/s over a voltage range of -1.0 to 1.5 V are shown in Fig. 4. Cyclic voltammetry revealed three anodic/cathodic peak couples. The first two pairs of redox peaks, located at 0.8/0.68 and 0.89/1.02 V (average redox potentials of 0.74 and 0.96 V vs. Ag/AgCl), respectively, were observed, due to intercalation/deintercalation of lithium ions from/into the manganese spinel phase²¹⁻²³, indicating that the oxidation and reduction of LiMn_2O_4 , occurs as shown in the following equation:



The other pair of redox peaks, located at -0.45 and 0.01 V (redox potential vs. Ag/AgCl), were also due to the Li-ion intercalation and deintercalation, indicating that the subsequent reduction and oxidation of LiMn_2O_4 occur as shown in the following equation:



For that reason, insertion/extraction of Li ions from the hosts before the evolution of oxygen and hydrogen is possible. The evolution of oxygen and hydrogen occur at about $E_{\text{Ag/AgCl}} = 1.3$ and -1.1 V, respectively which confirms that LiMn_2O_4 is stable in the aqueous electrolyte during the Li-ion intercalation and deintercalation. Accordingly, an aqueous rechargeable lithium ion battery (ARLB) can be prepared by using this sort of intercalation compound as both the anode and cathode electrodes. An inexpensive salt such as Li_2SO_4 can be used to replace the expensive LiPF_6 used in organic lithium ion batteries. In addition, the dry environment needed during the manufacturing of lithium ion batteries can be avoided.

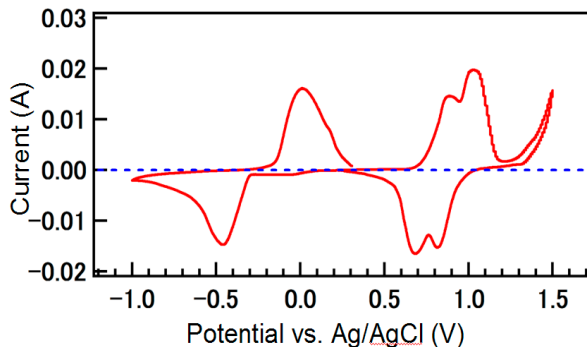


Fig. 4 Cyclic voltammogram of LiMn_2O_4 in $2 \text{ mol/dm}^3 \text{ Li}_2\text{SO}_4$ aqueous solution with a scanning rate of 0.5 mV/s .

We performed galvanostatic cycling experiments to evaluate the behavior of LiMn_2O_4 in an aqueous electrolyte containing $2 \text{ mol/dm}^3 \text{ Li}_2\text{SO}_4$ solution. A floating three-electrode configuration, which consisted of a Pt counter electrode, an Ag/AgCl reference electrode and a LiMn_2O_4 working electrode, was employed to characterize the electrochemical behaviors of a cathode. When the anode behavior of the electrode was examined, LiMn_2O_4 was also used as a counter electrode. In this case, LiMn_2O_4 acted as a reversible lithium source analogous to the lithium metal employed in the half cells, assembled with the organic electrolyte when the electrochemical behaviors of the individual electrodes were studied. Fig. 5 shows typical charge/discharge profiles of individual electrode vs. Ag/AgCl reference electrode. As a result of half-cell tests of the cathode and anode, the initial discharge capacities estimated were 104 and 112 mAh/g, respectively. It specified reversible intercalation and deintercalation of lithium ions in the aqueous electrolyte without the evolution of oxygen and hydrogen for both electrodes. Furthermore, the average voltage of a full cell could be predicted from the results of individual half cell tests. The potentials of the cathode (LiMn_2O_4) were 0.87 and 0.71 V vs. Ag/AgCl at the charge and discharge, correspondingly. In the case of the anode (LiMn_2O_4), potentials were located at -0.29 and -0.18 V vs. Ag/AgCl at the charge and discharge, respectively. Hence we could estimate that the charge and discharge potentials of the full cell should appear at 1.16 and 0.89 V, respectively.

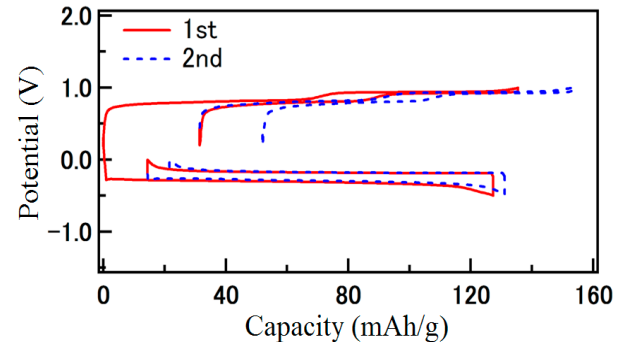


Fig. 5 Charge and discharge profiles of (a) cathode LiMn_2O_4 and (b) anode LiMn_2O_4 in $2 \text{ mol/dm}^3 \text{ Li}_2\text{SO}_4$ aqueous solution.

The charge/discharge performance of the $\text{Li}_{1-x}\text{Mn}_2\text{O}_4//\text{Li}_{1+x}\text{Mn}_2\text{O}_4$ cell with aqueous electrolyte has been determined at a current density of 50 mA/g over a potential range between 0.5 and 1.3 V, and the capacity was calculated based on the weight of the cathode active material. In the above-mentioned equations 3 and 4, during charging, the lithium ions were extracted from the LiMn_2O_4 cathode host, forming $\text{Li}_{1-x}\text{Mn}_2\text{O}_4$, and inserted into the LiMn_2O_4 anode, changing the composition to $\text{Li}_{1+x}\text{Mn}_2\text{O}_4$. In contrast, during discharge, lithium ions were extracted from the anode and inserted into the cathode. According to the potentials of both the cathode and anode electrodes, the cell should have a terminal voltage near 1.0 V. The charge/discharge profile is shown in Fig. 6. The initial capacity delivered was 110 mAh/g

with 88% coulombic efficiency. The average charge and discharge voltages were 1.1 and 0.9 V, respectively.

For comparison with the electrochemical behaviors of spinel LiMn_2O_4 , we performed the same experiment with the organic electrolyte composition $1 \text{ mol/dm}^3 \text{ LiPF}_6/\text{EC}:\text{DMC}$ (1:1 vol%) commonly used in non-aqueous LIBs. The cycling tests were carried out at various current densities. Fig. 7 shows the rate capability of $\text{Li}_{1-x}\text{Mn}_2\text{O}_4//\text{Li}_{1+x}\text{Mn}_2\text{O}_4$ with dependence on the electrolyte composition. The symmetric cell with LiMn_2O_4 using organic electrolyte shows good cycling performance at a current density of 0.2 mA/cm^2 . However, with increased current density, the advantages of an aqueous electrolyte became obvious. The symmetric spinel LiMn_2O_4 cell with aqueous electrolyte shows superior rate capability compared to that with organic electrolyte. At the current density higher than 1.0 mA/cm^2 , the capability of the organic electrolyte clearly decreased rapidly, while that of the aqueous electrolyte showed smooth changes. These results are supported by the superior ionic conductivity of aqueous electrolytes, which is usually two orders of magnitude higher than that of organic electrolytes. Fig. 8 shows the cycling behavior at 50 A/cm^2 between 0.5 and 1.3 V. Approximately 55 % of the maximum discharge capacity delivered on the first cycle was maintained after an additional 30 cycles. Naturally, capacity fades, but this can be slowed by adjusting the electrolyte composition by, for example, supplying different additives, modifying the electrode surface or controlling the pH, which will be the object of the next phase of our research.

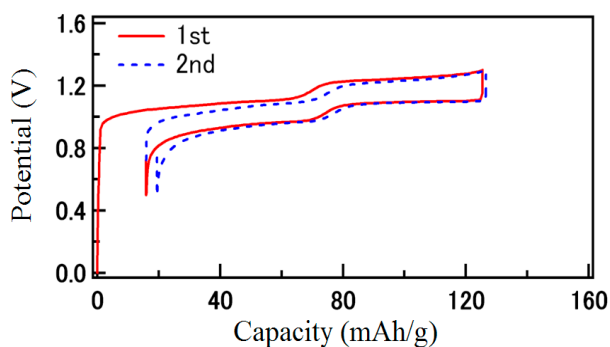


Fig. 6 Charge and discharge profile of $\text{Li}_{1-x}\text{Mn}_2\text{O}_4//\text{Li}_{1+x}\text{Mn}_2\text{O}_4$ with $2 \text{ mol/dm}^3 \text{ Li}_2\text{SO}_4$ aqueous solution.

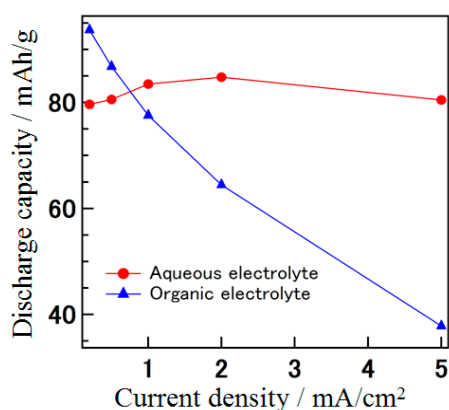


Fig. 7 Rate capability of symmetric cell with LiMn_2O_4 in different electrolyte.

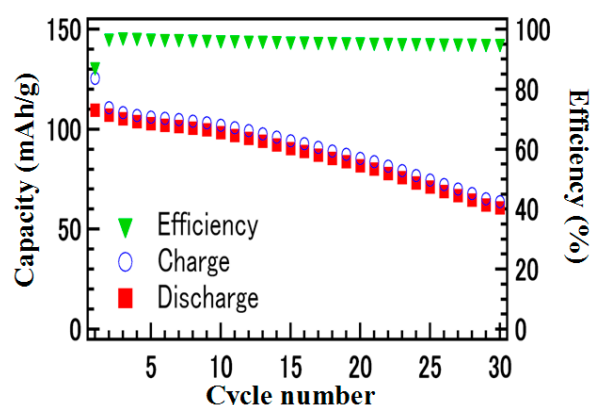


Fig. 8 Cyclability of symmetric cell with LiMn_2O_4 with $2 \text{ mol/dm}^3 \text{ Li}_2\text{SO}_4$ aqueous solution at 50 mA/cm^2 .

4. Conclusions

The electrochemical characteristics of LiMn_2O_4 used as both the cathode and the anode in a symmetric cell were studied in $2 \text{ mol/dm}^3 \text{ Li}_2\text{SO}_4$ aqueous electrolyte with respect to its use as a new kind of rechargeable battery system. Cyclic voltammetry showed that spinel LiMn_2O_4 reversibly intercalated/deintercalated Li^+ ions at potentials far below the potentials of hydrogen and oxygen evolution in an aqueous solution with $\text{pH}=7$. The symmetric spinel battery delivers about 110 mAh/g discharge capacity, based on the mass of the cathode electrode. It is important that the rate capability of the LiMn_2O_4 with aqueous electrolyte was found to be preferable to that with organic electrolyte composition. The pilot results show that the symmetric aqueous electrochemical system has promising characteristics, since this kind of battery is extremely safe for large-scale energy storage and conversion. The ionic conductivity of aqueous electrolyte is higher than that of organic electrolyte, which contributes to the high rate capability. In addition, the cost of the aqueous cell will be lower than that of previous cell designs, because electrode and electrolyte materials are not expensive compared with those used in conventional lithium ion batteries. Furthermore, the assembling process is simple and trouble-free, and it does not require strict control of humidity and the environment.

Acknowledgements: This work was supported by Global-Centre of Excellence in Novel Carbon Resource Sciences, Kyushu University.

References

- 1) K. Zaghib, K. Striebel, A. Guerfi, J. Shim, M. Armand, M. Gauthier, *Electrochem Acta*, **50**, 263 (2004).
- 2) K. Zaghib, J. Shim, A. Guerfi, P. Charest, K. A. Striebel, *Electrochem. Solid State Lett.*, **8**, A207 (2005).
- 3) T. Lam, R. Louey, *J. Power Sources*, **158**, 1140 (2006).
- 4) A. W. Stienecker, T. Stuart, C. Ashtiani, *J. Power Sources*, **156**, 755 (2006).
- 5) C. Deng, P. F. Shi, S. Zhang, *Electrochem. Solid State Lett.*, **9**, A303 (2006).
- 6) T. Horiba, K. Hironaka, T. Matsumura, *J. Power Sources*, **119**, 893 (2006).

- 7) K. Smith, C. Y. Wang, *J. Power Sources*, **161**, 628 (2006).
- 8) K. Smith, C. Y. Wang, *J. Power Sources*, **160**, 662 (2006).
- 9) I. Belharouak, W. Q. Lu, D. Vissers, K. Amine, *Electrochem. Commun.*, **8**, 329 (2006).
- 10) J. Kohler, H. Makihara, H. Uegaito, H. Inoue, M. Toki, *Electrochim. Acta*, **46**, 59 (2000).
- 11) Y. G. Wang, Y. Y. Xia, *Electrochem. Commun.*, **7**, 1138 (2005).
- 12) G. X. Wang, S. Zhong, D.H. Bradhurst, S. X. Dou, H. K. Liu, *J. Power Source*, **74**, 198 (1998).
- 13) N. C. Li, C. J. Patrissi, G. L. Che, C. R. Martin, *J. Electrochem. Soc.*, **147**, 2044 (2000).
- 14) W. Li, J. R. Dahn, D. S. Wainwright, *Science*, **264**, 1115 (1994).
- 15) W. Li, J. R. Dahn, *J. Electrochem. Soc.*, **142**, 1742 (1995).
- 16) X. H. Liu, T. Saito, T. Doi, S. Okada, J. I. Yamaki, *J. Power Sources*, **189**, 706 (2009).
- 17) J. Y. Luo and Y. Y. Xia, *Advanced Functional Materials*, **17**, 3877 (2007).
- 18) Y. S. Lee, Y. K. Sun, K. S. Nahm, *Solid State Ionics*, **109**, 285 (1998).
- 19) [19] M. M. Thackeray, A. de Kock, M. H. Rossouw, D. Liles, R. Bittihm, D. Hodge, *J. Electrochem. Soc.*, **139**, 363 (1992).
- 20) M. Jayalakshmi, M. Mohan Rao, *J. Power Sources*, **157**, 624 (2006).
- 21) D. Guyomard, J.M. Tarascon, *J. Electrochem. Soc.*, **139**, 937 (1992).
- 22) T. Ohzuku, M. Kitagawa, T. Hirai, *J. Electrochem. Soc.*, **137**, 769 (1990).
- 23) A. H. Gemeay, H. Nishiyama, S. Kuwabata, H. Yoneyama, *J. Electrochem. Soc.*, **142**, 4190 (1995).